Sensors and Actuators B 245 (2017) 183–188

Contents lists available at ScienceDirect

Sensors and Actuators B: Chemical

journal homepage: www.elsevier.com/locate/snb

A high-integration sensor array sensitive to oxynitride mixture

Zhigang Pan[a], Yong Zhang[a,*], Zhenzhen Cheng[a], Bingdian Liang[a], JingYuan Zhang[a], Xin Li[b], Xiaohua Wang[a], Dingxin Liu[a], Aijun Yang[a], Mingzhe Rong[a], Xiaowen Chen[c]

[a] State Key Laboratory of Electrical Insulation and Power Equipment, Xi'an Jiaotong University, Xi'an,710049, China
[b] Vacuum Micro-Electronic & Micro-Electronic Mechanical Institute, School of Electronics and Information Engineering, Xi'an Jiaotong University, Xi'an, 710049, China
[c] HuangHe Hydropower Development CO., LTD., Xining, 810008, China

ARTICLE INFO

Article history:
Received 26 May 2016
Received in revised form
24 November 2016
Accepted 20 January 2017
Available online 23 January 2017

Keywords:
Oxynitride
Gas mixture
Sensor array
Carbon nanotubes
Gas discharge

ABSTRACT

Measuring the concentration of oxynitride NO_x (including NO and NO_2) can provide a scientific basis for determining its potential harm to the human body. The existing metal oxide semiconductor sensor arrays are greatly limited by high operating temperature and low integration. In this article, we report on a high-integration carbon nanotubes sensor array with two different electrode separations sensitive to oxynitride mixture at low temperature. The triple-electrode sensor array is comprised of a large carbon nanotube array cathode, two extracting electrodes and two collecting electrodes and worked at non-self-sustaining discharge state, which was determined by the study on current-voltage characteristic of a double-electrode structure sensor. Through studying the relationship between gas concentration and discharge current at 1 atm, we obtained the distinct sensitivities of the binary mixture in the concentration ranges of 0–1166 ppm NO and 0–712 ppm NO_2 using the sensor array at low operating voltages and 60 °C. Collecting currents of the two sensors in the array decreased with increasing NO and NO_2 concentration in the gas mixture. The repeatable characteristics and dynamical response tests of the sensors were also conducted. The proposed sensor array has potential for the direct detection of a NO-NO_2 mixture without separating the mixed gases.

1. Introduction

As a major source of air pollution, NO_x (NO and NO_2) would not only cause great harms on the environment, but also generate harmful secondary particles like $PM_{2.5}$ and PM_{10} through physical and chemical reactions. Therefore, measuring concentration of NO-NO_2 mixture is of great significance.

The chromatography is a kind of traditional accurate monitor for gas mixture detection, but has the drawbacks of being very bulky and costly [1,2]. The metal oxide semiconductor sensor array has been reported for detecting gas mixture [3–5], but have been limited by several disadvantages like operating at high temperature (>300 °C) [6], and easy saturation [7,8]. For the past several years, carbon nanotubes (CNTs) have been considered as promising candidates for sensing materials to NO and NO_2 [9–11]. A chemical sensor based on individual single-walled carbon nanotubes was designed and its resistance decreased when it was exposed to 200 ppm NO_2 at room temperature [9]. Ueda et al. [10] fabricated a carbon nanotube based thin film NO sensor and the resistance of the sensor decreased when the NO concentration increased from 50 ppm (1 ppm = 1 μL/L) to 100 ppm at various given temperature values in a range of 25–250 °C. A multi-walled CNTs (MWCNTs) based gas sensor treated by laser irradiation showed better response than the unirradiated to 0–10 ppm NO at 150 °C [11]. The above sensors based on adsorption have been limited by narrow measuring range and a long time to response and recover (0.5–30 min) [7–9]. Ionization sensors using carbon nanotubes overcome the limitations above and exhibite low operating voltage, wider measuring range, lower operating temperature and fast response [12–18]. In this paper, we chose two different electrode separations for fabricating a two triple-electrode sensors array with carbon nanotubes grown on one cathode by using Microelectro Mechanical Systems (MEMS) technology, and conducted tests at low temperature and low operating voltage for detecting the two components of NO and NO_2 in a mixture with N_2 and synthetic air without component separation. The repeatable characteristics, dynamical response and the relation between the sensing response and the environment temperature tests of the sensors were also conduct for application.

* Corresponding author.
E-mail address: zhyong@mail.xjtu.edu.cn (Y. Zhang).

http://dx.doi.org/10.1016/j.snb.2017.01.115
0925-4005/

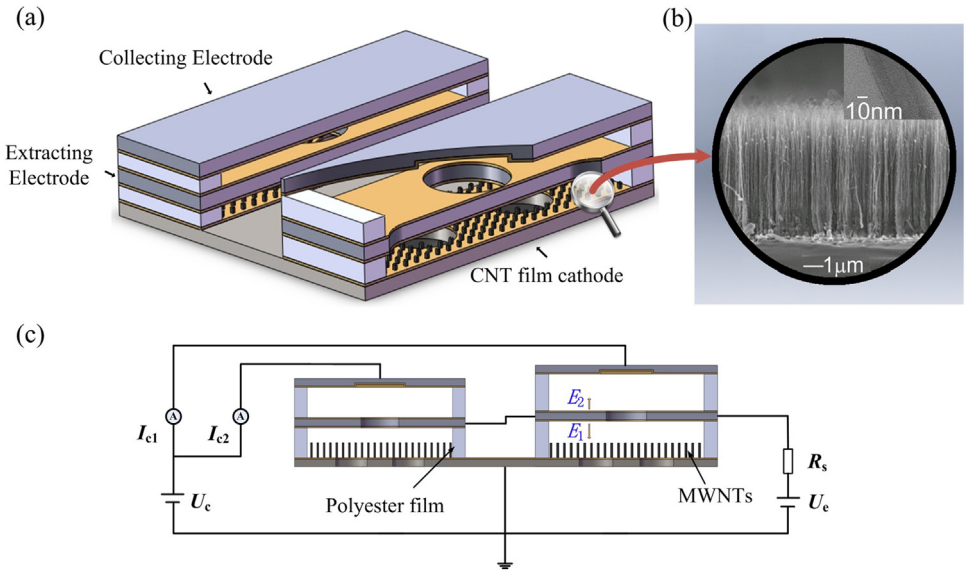

Fig. 1. The sensor array device. (a) Three-dimensional schematic of the device structure; (b) SEM micrograph of the carbon nanotubes; (c) Diagram of the actual test set-up.

2. Experimental details

Fig. 1 shows the details of our triple-electrode sensor array, which is comprised of two sensors with a large carbon nanotube array cathode (500 μm thick, 27 mm in length, 24 mm in width), two extracting electrodes and two collecting electrodes (500 μm thick, 27 mm in length, 8 mm in width). 50 nm thick Ti film, 400 nm thick Ni film and 125 nm thick Au film were sputtered on the both sides of the two extracting electrodes and the inner side of the cathode and two collecting electrodes. Then the five electrodes were rapidly annealed in a low vacuum of ~3.0 Pa at 450 °C for 50 s to alloy the Ti/Ni/Au film. The multiwalled nanotube (MWNT) array was grown by thermal chemical vapor deposition (TCVD) [19,20] on the inner side of the cathode. The nanotubes in the film are ~40 nm in diameter, and ~5–6 μm in length (Fig. 1b). The carbon nanotubes between the two sensors were removed by adhesive transfer method [21]. The distances between the cathode and the extracting electrode, and between the extracting and the collecting electrodes are the same. One sensor with 100 μm separations in the sensor array detected NO in a 0–1166 ppm range, and the other sensor with 120 μm separations detected NO_2 in a 0–712 ppm range. Controlled d.c. voltages of U_e and U_c (NI PXI-4132) are applied between the cathode and the extracting electrodes, and between the cathode and the collecting electrodes (Fig. 1b), respectively. U_e is higher than U_c, which generates two electric fields E_1 and E_2 in reversed field direction. The collecting currents I_{c1} and I_{c2} are measured by two digital multimeters (NI PXI-4071), and the resistor R_s is used to limit extracting current.

First, the effect of gas concentration on collecting current was studied. The sensor array was placed in a sensing cell (Fig. 2). Before the measurements, temperature was increased to 60 °C within 1 min by a temperature control device, and then the air was pumped out of the chamber by vacuum pump to establish a low vacuum with a gas pressure of 5 kPa. There were three gas cylinders containing high purity gas with concentration accuracy of 2%. One of them supplied the 99.999% environment gas N_2 and the others supplied the 0.5% NO and the 0.5% NO_2. Three mass flow controllers (MFC1, MFC2 and MFC3, Line Tech M3030 V with 1% accuracy) were used to continuously regulate gas flux for preparing the mixed gas concentrations. The full scales of the three MFCs were 1000 mL/min, 50 mL/min, 100 mL/min, respectively. After well mixed in a gas mixing chamber, gas mixture flowed into a sealable stainless steel sensing cell with a pressure meter to monitor gas pressure. Sixteen samples were tested while NO_2 concentration increased from 0 to 712 ppm at various given NO concentrations in a range of 0–1166 ppm.

3. Results and discussion

The working state of the triple-electrode sensors in the array is distinct from that of traditional double-electrode breakdown gas sensors [16–18]. Fig. 3 shows the current–voltage characteristic of a double-electrode sensor with 120 μm electrode separation in nitrogen at 1 atm and 23.7 °C. Non-self-sustaining discharge happened first, and then self-sustaining discharge developed, and a discharge current of 1.44 mA generated at the operating voltage of 350 V between the two electrodes. The carbon nanotubes were damaged due to the high discharge current density up to 474 A/m^2 with the area of CNTs calculated as 3.04×10^{-6} m^2, which would lead to a short operating life [22]. Therefore, the sensors using CNTs should keep working at non-self-sustaining discharge state by applying voltage below the breakdown voltage (350 V), which can reduce power consumption and extend the life-span of the sensors.

To understand the effect of electric field distribution and electrode separation as well as gas concentration on gas discharge current, analysis follows: The electric field E_{tip} near carbon nanotube tip is higher than the average electric field E_1 because of the high aspect ratio and the small radius of the curvature. The rate E_{tip}/E_1 is called an electric field enhancement factor γ and estimated according to the morphology of carbon nanotubes[23],

$$\gamma = 3 + 2(1+\eta)/\{(2+\eta)[2\pi(2+\eta)\delta^2 + \eta]\} \quad (1)$$

$$\eta = \rho/h \quad (2)$$

$$\delta = \rho/D \quad (3)$$

where ρ is the radius of a carbon nanotube, h is the height of a carbon nanotube, and D is the distance between the nearest carbon nanotube. According to Fig. 1b, ρ=20 nm, h = 6 μm, D = 100 nm, and then γ=5, E_{tip} = 5E_1. The enhanced E_{tip} could increase the number of the electrons emitted from the cathode [24]. The electrons collide with gas molecules, and most electrons and positive ions are produced near the tips. Through collision and diffusion, significant amount of the positive ions overcome the weak field E_1 near the extracting electrode and move into the region between the extract-

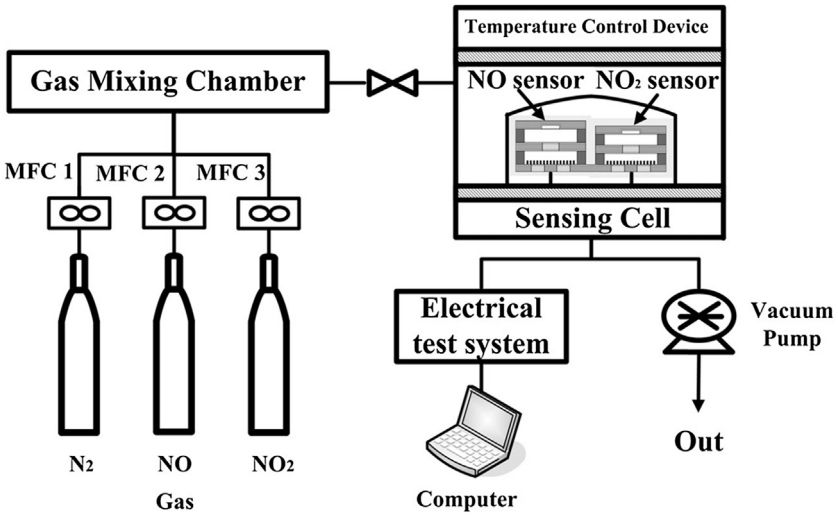

Fig. 2. Schematic view of the experimental set-up.

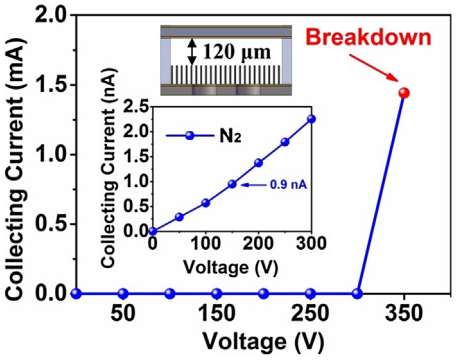

Fig. 3. *I–V* characteristics of the double-electrode CNT sensor with 120 μm electrode separations in nitrogen.

ing and the collecting electrodes, then they are accelerated by E_2 towards the collecting electrode as the collecting current I_c. The collecting current I_c is a part of the total discharge current I [25],

$$I = I_0 e^{\alpha d} \tag{4}$$

where I_0 is initial current, d is electrode separation between cathode and extracting electrode, α is the first ionization coefficient and reflects ionization ability of gas from collision with electrons,

$$\alpha = APe^{-BP/E} \tag{5}$$

where A and B are constants related to gas species and temperature, E is the applied electric field, P is the partial pressure proportional to the gas concentration φ when the gas temperature and the volume are constant at 1 atm. It shows that the collecting current is varied at different electrode separation d and gas concentrationφ.

Since the collecting current I_c is an exponential function of the electrode separation d and the gas concentrationφ, I_c will be different at various electrode separations d. Therefore, we chose two different electrode separations of d_1 and d_2 for fabricating two sensors to constitute an array, and conducted tests for studying the relationship between collecting currents and concentrations of NO and NO_2 (Eqs. (6) and (7)).

$$I_{c1} = f_1(d_1, \varphi_{NO}, \varphi_{NO2}) \tag{6}$$

$$I_{c2} = f_2(d_2, \varphi_{NO}, \varphi_{NO2}) \tag{7}$$

where I_{c1} and I_{c2} are collecting current, the function f_1 in Eq. (6) describes the effect of d_1, φ_{NO} and φ_{NO2} on I_{c1}; f_2 in Eq. (7) describes the effect of d_2, φ_{NO} and φ_{NO2} on I_{c2}. When the electrode separations of two sensors are given, the concentrations of NO_2 and NO mixed with N_2 can be detected without component separation.

One sensor with 100 μm separations detected NO in a 0–1166 ppm range, and the other sensor with 120 μm separations detected NO_2 in a 0–712 ppm range, wider than that of the existing sensors based on CNTs [9–13]. The collecting currents were measured and showed as single-valued functions of two component concentrations (Fig. 4). The maximum standard deviation values are 0.14 nA at 0 ppm NO and NO_2 (Fig. 4a) and 0.04 nA at 0 ppm NO_2/833 ppm NO (Fig. 4b), which display smaller variation coefficients of 2.91% (Fig. 4a) and 4.7% nA (Fig. 4b), respectively. Collecting currents of the NO sensor monotonically decreased with NO concentration increasing from 0 to 1166 ppm (Fig. 4a), and the four curves were varied at different NO_2 concentrations, exhibiting the highest sensitivity of −1.4 pA/ppm to 305 ppm NO. The collecting currents of the NO_2 sensor also monotonically decreased with NO_2 concentration increasing from 0 to 712 ppm (Fig. 4b), and the four curves were varied at different NO concentrations, exhibiting the highest sensitivity of −4 pA/ppm to 194 ppm NO_2, three orders higher than that of the NO sensor. It shows that the collecting current values of the two sensors with 100 μm and 120 μm separations are completely different at the same gas mixture (Fig. 4c).

Fig. 4a and b show the effect of NO_2 concentration on NO detection and that of NO concentration on NO_2 detection, respectively, which is cross sensitivity phenomenon between NO and NO_2. We found that the collecting current of the NO sensor decreased from 2.82 to 0.44 nA when the measured NO concentration does not change and keeps as 305 ppm, but NO_2 concentration changes from 0 to 712 ppm (Fig. 4a). Similarly, the collecting current of the NO_2 sensor decreased from 0.58 to 0.35 nA when the measured NO_2 concentration does not change and keeps as 194 ppm, but NO concentration changes from 0 to 1166 ppm (Fig. 4b). The cross sensitivity $S_{x\text{-}y}$ between NO and NO_2 is calculated to estimate the effect between the two components,

$$S_{x\text{-}y} = \Delta I_{cm} \div (I_{cFS} \times \Delta\varphi_y) \tag{8}$$

where ΔI_{cm} is the maximum deflection of collecting current of the x sensor at given concentrations and a given concentration change $\Delta\varphi_y$ of the y component, and I_{cFS} is the maximum deflection between the maximum and minimum collecting currents of the x sensor. The highest cross sensitivity of the NO sensor to NO_2 is -2.9×10^{-3} ppm^{-1} at 305 ppm NO, one order higher than that of the NO_2 sensor to NO, -1.4×10^{-4} ppm^{-1} at 194 ppm NO_2, indicat-

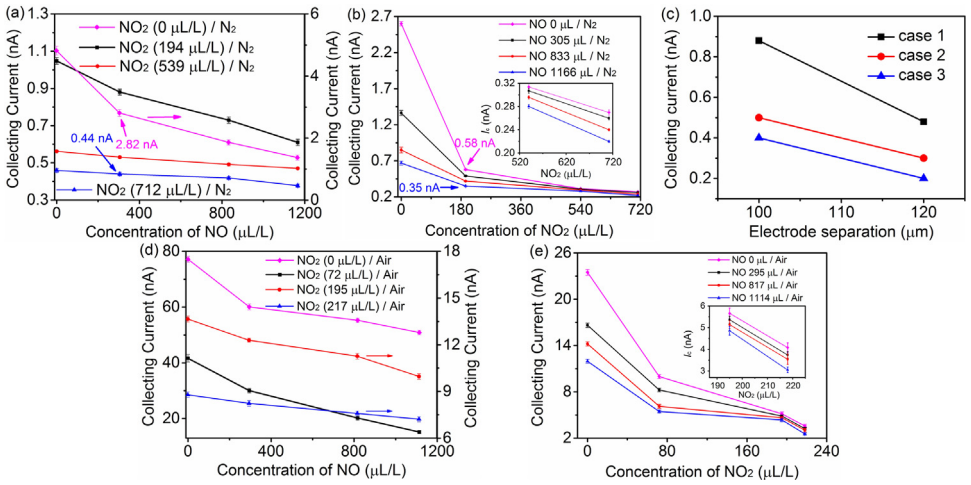

Fig. 4. Simultaneous detection of a NO-NO_2 mixture by using a sensor array with 100 μm and 120 μm separations at 150 V U_e and 10 V U_c. Collecting current decreases with increasing (a) NO and (b) NO_2 concentrations in N_2. (c) Collecting current comparison of two sensors with 100 μm and 120 μm separations in N_2. Case 1 denotes a concentration in a gas mixture of NO (305 ppm)/NO_2 (194 ppm), 2 of NO (833 ppm)/NO_2 (540 ppm), 3 of NO (1166 ppm)/NO_2 (712 ppm). It shows that two separations enable completely different collecting currents. Collecting current also decreases with increasing (d) NO and (e) NO_2 concentrations in synthetic air.

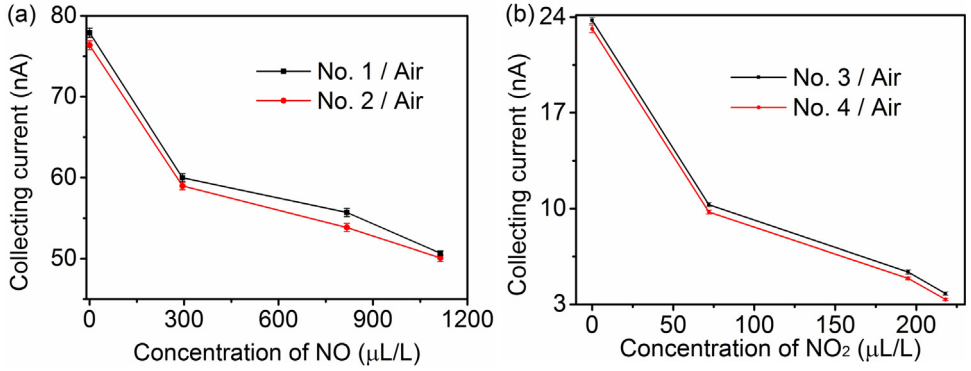

Fig. 5. The repeatable single-valued characteristics of the sensors in synthetic air at 150 V U_e and 10 V U_c. Sensitivity curves of (a) Nos. 1 and 2 of the 100 μm separation sensor to NO and (b) Nos. 3 and 4 of the 120 μm separation sensor to NO_2, exhibiting the repeatable single-valued characteristics of the sensor array in synthetic air.

Table 1
Considered reaction processes.

No.	Reaction	Rate constant[a] ($cm^3\ s^{-1}$)	Reference
R1	$e + N_2 \rightarrow N_2(A^3\sum_u^+) + e$	$f(T_e)$	[26]
R2	$e + N_2 \rightarrow N_2(a'^1\sum_u^-) + e$	$f(T_e)$	[26]
R3	$N_2(A^3\sum_u^+) + N_2(a'^1\sum_u^-) \rightarrow N_2 + N_2^+ + e$	5.0×10^{-11}	[26]
R4	$N_2(a'^1\sum_u^-) + N_2(a'^1\sum_u^-) \rightarrow N_2 + N_2^+ + e$	2.0×10^{-10}	[26]
R5	$N_2(A^3\sum_u^+) + N_2(a'^1\sum_u^-) \rightarrow N_4^+ + e$	5.0×10^{-11}	[26]
R6	$N_2(a'^1\sum_u^-) + N_2(a'^1\sum_u^-) \rightarrow N_4^+ + e$	2.0×10^{-10}	[26]
R7	$N_2(A^3\sum_u^+) + NO \rightarrow N_2 + NO$	5.5×10^{-11}	[27]
R8	$N_2(a'^1\sum_u^-) + NO \rightarrow N_2 + N + O$	3.6×10^{-10}	[27]
R9	$N_2(A^3\sum_u^+) + NO_2 \rightarrow N_2 + NO + O$	1.3×10^{-11}	[27]
R10	$N_2(a'^1\sum_u^-) + NO \rightarrow N_2(X) + N + O$	3.3×10^{-10}	[28]

[a] Rate constant denotes the number of events per unit time per electron and per molecule, $f(T_e)$ indicates that the rate constant could obtained from electron energy distribution function (EEDF) using cross sections.

ing a stronger effect of NO_2 on NO detection than that of NO on NO_2 detection. It shows that the ionization gas sensor is more sensitive to NO_2 than to NO. In order to reduce the cross sensitivity between NO and NO_2 components, the two functions g_1 and g_2 could be established through proper data fusion [4,5], then the calculated concentration φ'_{NO} and φ'_{NO2} could be obtained ($\varphi'_{NO} = g_1(I_{c1}, I_{c2})$, $\varphi'_{NO2} = g_2(I_{c1}, I_{c2})$).

We also used the sensor array with 100 μm and 120 μm separations to detect oxynitride mixture in synthetic air, respectively. Single-valued sensitivities were found at 150 V U_e and 10 V U_c (Fig. 4d and e). Fig. 5 displays two adjacent sensitivity curves for NO (Fig. 5a) and NO_2 (Fig. 5b), respectively, exhibiting our finding on the reproducible characteristic of the sensors in NO and NO_2.

The single-valued decreases of collecting currents (Fig. 4) were analyzed as follows. There are mainly ten reaction processes (Table 1) occurred in the gas mixture discharge. In the mixture with N_2, the two excited metastable states of N_2, $N_2(A^3\sum_u^+)$, and $N_2(a'^1\sum_u^-)$ could be strongly populated through R1 and R2, due to

their lower excitation energies of 6.2 eV and 8.4 eV than the ionization energies of NO and NO_2 with 9.25 eV and 9.8 eV, respectively [26]. Therefore, the positive ions are mainly generated through the associative ionizations R3–R6 between the two metastable states. Simultaneously, the two metastable states $N_2(A^3\sum u^+)$, and $N_2(a'^1\sum u^-)$ are significantly consumed through the quenching reactions R7–R10 by NO and NO_2, which generate some neutral particles like metastable state $N_2(X)$ [27,28]. Consequently, the number of the positive ions decreases with increasing NO_x concentration.

The dynamical response test of the sensor was conducted. Herein, we define the response and recovery time as the time required to reach 90% of the total change [29–31]. The response and recovery characteristics of the sensor to 1114 ppm NO in synthetic air with ~79% N_2 and 21% O_2 were studied (Fig. S1), and around 9 s and 6 s were estimated as the maximum values of the response and recovery time, respectively. Since temperature has effect on gas ionization, temperature test was conducted in a range of 30–70 °C (Fig. S2). Collecting current I_c of the 120 μm sensor exhibits an exponential increase with temperature at 150 V U_e and 10 V U_c. I_c increases from 1.27 nA to 2.49 nA by an increment of 1.27 nA when temperature rises from 50 °C to 60 °C. Therefore, temperature effect cannot be ignored, and the sensors in the array worked at a constant temperature. In our later study, a different interelectrode separation sensor was used to monitor the temperature and could compensate the relevant effect.

4. Conclusion

In this article, we report on a carbon nanotubes sensor array sensitive to NO-NO_2 mixture. The sensor array is comprised of two sensors with a large carbon nanotube array cathode, two extracting electrodes and two collecting electrodes. The two sensors in the array had shown distinct collecting currents when exposed to various concentrations of the NO-NO_2 mixture in N_2. Eight single-valued sensitivity curves were directly obtained at low voltage and low temperature. The sensor array exhibits high integration, wider measuring range, lower operating voltages, good reproducibility and rapid response time. It shows that the two-sensor array has the potential to detect the NO and NO_2 components without separating the mixture.

Acknowledgments

We thank W. H. Jiang and J. Wang for contributions to the experiments. This work is partially supported by the Specialized Research Fund for the Doctoral Program of Higher Education (20130201110007), the Natural Science Basic Research Plan in Shaanxi Province of China (2014JZ017), the Director Fund (EIPE14125) of the State Key Lab of Electrical Institution and Power Equipment of Xi'an Jiaotong University, the Fundamental Research Funds (xkjc2015012) for the Central Universities, and the National Natural Science Foundation of China (51577142). We thank International Center for Dielectric Research of Xi'an Jiaotong University, Xi'an, China.

Appendix A. Supplementary data

Supplementary data associated with this article can be found, in the online version, at http://dx.doi.org/10.1016/j.snb.2017.01.115.

References

[1] J. Rudnicka, M. Walczak, T. Kowalkowski, T. Jezierski, B. Buszewski, Determination of volatile organic compounds as potential markers of lung cancer by gas chromatography–mass spectrometry versus trained dogs, Sens. Actuators B 202 (2014) 615–621.
[2] S.Y. Oh, Fast gas chromatography–surface acoustic wave sensor: an effective tool for discrimination and quality control of lavandula species, Sens. Actuators B 182 (2013) 223–231.
[3] B.J. Kim, J.S. Kim, Gas sensing characteristics of MEMS gas sensor arrays in binary mixed-gas system, Mater. Chem. Phys. 138 (2013) 366–374.
[4] L. Zhang, F. Tian, X. Peng, X. Yin, G. Li, L. Dang, Concentration estimation of formaldehyde using metal oxide semiconductor gas sensor array-based e-noses, Sens. Rev. 34 (2014) 284–290.
[5] J. Fonollosa, I. Rodriguez-Lujan, A.V. Shevade, M.L. Homer, M.A. Ryan, R. Huerta, Human activity monitoring using gas sensor arrays, Sens. Actuators B 199 (2014) 398–402.
[6] C.C. Liu, J.H. Li, C.C. Chang, Y.C. Chao, H.F. Meng, S.F. Horng, H.H. Cheng, T.C. Meng, Selective real-time nitric oxide detection by functionalized zinc oxide, J. Phys. D: Appl. Phys. 42 (2009) 155105.
[7] E. Comini, G. Faglia, G. Sberveglieri, UV light activation of tin OxideThin films for NO2 sensing at low temperatures, Sens. Actuators B 78 (2001) 73–77.
[8] S. Zhuiykov, N. Miura, Development of zirconia-based potentiometric NOx sensors for automotive and energy industries in the early 21st century: what are the prospects for sensors? Sens. Actuators B 121 (2007) 639–651.
[9] J. Kong, N.R. Franklin, C. Zhou, M.G. Chapline, S. Peng, K. Cho, H. Dai, Nanotube molecular wires as chemical sensors, Science 287 (2000) 622–625.
[10] T. Ueda, H. Norimatsu, M.M.H. Bhuiyan, T. Ikegami, K. Ebihara, NO sensing property of carbon nanotube based thin film gas sensors prepared by chemical vapor deposition techniques, Jpn. J. Appl. Phys. 45 (2006) 8393–8397.
[11] T. Ueda, S. Katsuki, N.H. Abhari, T. Ikegami, F. Mitsugi, T. Nakamiya, Effect of laser irradiation on carbon nanotube films for NOx gas sensor, Surf. Coat. Tech. 202 (2008) 5325–5328.
[12] Y. Zhang, S.T. Li, J.Y. Zhang, Z.G. Pan, D.M. Min, X. Li, X.P. Song, J.H. Liu, High-performance gas sensors with temperature measurement, Sci. Rep-UK 3 (2013) 1267.
[13] J.Y. Zhang, Y. Zhang, Z.G. Pan, S. Yang, J.H. Shi, S.T. Li, D.M. Min, X. Li, X.H. Wang, D.X. Liu, A.J. Yang, Properties of a weakly ionized NO gas sensor based on multi-walled carbon nanotubes, Appl. Phys. Lett. 107 (2015) 093104.
[14] S.B. Cai, Y. Zhang, Z.M. Duan, Fabrication of gas sensor based on field ionization from SWCNTs with tripolar microelectrode, J. Micromech. Microeng. 22 (2012) 125017.
[15] S.B. Cai, Z.M. Duan, Y. Zhang, Flammable and noxious gas sensing using a microtripolar electrode sensor with diameter and chirality sorted single-walled carbon nanotubes, J. Micromech. Microeng. 23 (2013) 085022.
[16] A. Modi, N. Koratkar, E. Lass, B.Q. Wei, P.M. Ajayan, Miniaturized gas ionization sensors using carbon nanotubes, Nature 24 (2003) 171–174.
[17] Y. Zhang, J.H. Liu, C.C. Zhu, Novel gas ionization sensors using carbon nanotubes, Sens. Lett. 8 (2010) 219–227.
[18] Y. Zhang, J.H. Liu, X. Li, X.J. Tang, C.C. Zhu, Study of improving identification accuracy of carbon nanotube film cathode gas sensor, Sens. Actuators A-Phys. 125 (2005) 15–24.
[19] X. Li, J.H. Liu, Y. Zhang, J.Y. Dou, W.H. Liu, C.C. Zhu, C. Chang, Study of catalyst grains effect on electrode of self-sustaining dischargecarbon nanotubes gas sensor array, in: Proc. Int. Vac. Microelectron. Conf., USA, 2001, pp. 65–66.
[20] X. Li, J.H. Liu, J.Y. Dou, W.H. Liu, C.C. Zhu, Improvement of purity and field emission character of carbon nanotubes film by optimizing the density of thecatalyst solution, Chin. J. Xi'an Jiaotong Univ. 36 (2002) 1041–1044.
[21] Y. Zhu, X. Lim, M.C. Sim, C.T. Lim, C.H. Sow, Versatile transfer of aligned carbon nanotubes with polydimethylsiloxane as the intermediate, Nanotechnology 19 (2008) 714–721.
[22] X.H. Liang, S.Z. Deng, N.S. Xu, J. Chen, N.Y. Huang, J.C. She, Noncatastrophic and catastrophic vacuum breakdowns of carbon nanotube film under direct current conditions, J. Appl. Phys. 101 (2007) 63309.
[23] A.I. Zhbanov, E.G. Pogorelov, Y.C. Chang, Y.G. Lee, Screened field enhancement factor for the floating sphere model of a carbon nanotube array, J. Appl. Phys. 110 (2011) 114311.
[24] Y. Song, D.H. Shin, S.G. Jeon, J.I. Kim, C.J. Lee, Field emission properties of carbon nanotube emitters dependent on electrode geometry, J. Vac. Sci. Technol. B 31 (2013) 052203.
[25] M. Adel-Salam, High-Voltage Engineering: Theory and Practice, Dekker, New York, 2000.
[26] H. Brunet, S.J. Rocca, Model for a glow discharge in flowing nitrogen, J. Appl. Phys. 57 (1985) 1574–1581.
[27] G.B. Zhao, X. Hu, M.D. Argyle, M. Radosz, N atom radicals and N2 (A3$\sum$u+) found to Be responsible for nitrogen oxides conversion in nonthermal nitrogen plasma, Ind. Eng. Chem. Res. 43 (2004) 5077–5088.
[28] F. Fresnet, G. Baravian, L. Magne, S. Pasquiers, C. Postel, V. Puech, A. Rousseau, Influence of water on NO removal by pulsed discharge in N2/H2O/NO mixtures, Plasma Sources Sci. Technol. 11 (2002) 152.
[29] J. Fraden, Handbook of Modern Sensors, Springer, New York, 2010.
[30] L. Yang, H.T. Ban, M.J. Yang, Highly sensitive NH3 gas sensors based on novel polypyrrole-coated SnO2 nanosheet nanocomposites, Sens. Actuators B 224 (2016) 449–457.
[31] J. Guo, J. Zhang, H. Gong, D. Ju, B. Cao, Au nanoparticle-functionalized 3D SnO2: microstructures for high performance gas sensor, Sens. Actuators B 226 (2015) 266–272.

Biographies

Zhigang Pan is a doctoral student of School of Electrical Engineering of Xi'an Jiaotong University (XJTU), China. His research interest is sensing technology and system.

Yong Zhang is a professor of School of Electrical Engineering of Xi'an Jiaotong University (XJTU), China. She received her Ph. D. in XJTU in 2004. From 2010 to the present, she has been regular researcher in National Key Laboratory of Electrical Equipment and Electrical Insulation of XJTU. In 2014, she became an IEEE senior member. Her research interests include Intelligent sensor system, Nanometer sensor system, Modern measurement and control instruments, Multi-information fusion technology of multi-sensors and Diagnostic technology of gas discharge plasma.

Zhenzhen Cheng is a doctoral student of School of Electrical Engineering of Xi'an Jiaotong University, China. Her research interest is nanosensor and multiple sensor data fusion.

Bingdian Liang is a master student of School of Electrical Engineering of Xi'an Jiaotong University (XJTU), China. His research interest is gas sensor and intelligent sensor system.

Jingyuan Zhang is a doctoral student of School of Electrical Engineering of Xi'an Jiaotong University, China. Her research interest is intelligent sensor technology and sensor device.

Xin Li is an associate professor of Department of Microelectronics at Xi'an Jiaotong University. She has wide-ranging interests in Carbon-based Nanomaterials devices and Bio Nanoelectronics.

Xiaohua Wang is a professor of School of Electrical Engineering of Xi'an Jiaotong University (XJTU), China. His main research interest is condition monitoring of electrical machines, plasma physics and intelligent electrical apparatus and key technology.

Dingxin Liu is an associate professor of School of Electrical Engineering of Xi'an Jiaotong University (XJTU), China. His main research interest is theoretical insight into low-temperature atmospheric-pressure plasmas and intelligent electrical apparatus and key technology.

Aijun Yang is a lecturer of School of Electrical Engineering of Xi'an Jiaotong University (XJTU), China. His main research interest is electrical & electronics engineering, plasma and MATLAB simulation.

Mingzhe Rong is professor of School of Electrical Engineering of Xi'an Jiaotong University (XJTU), China. He was awarded the Distinguished Professor for Yangtze River Scholar Project in XJTU. He is a member of the Disciplinary Assessment Team for Electric Engineering of Academic Degree Commission of the State Council. His major fields of scientific research include Basic theories and application of electric equipment, switch simulation analysis based on coupled simulation of multiple physical fields and electrical arc magnet fluid dynamics model, condition monitoring and faults diagnosis of electric equipment, etc.

Xiaowen Chen is a senior engineer of HuangHe Hydropower Development CO., LTD., China. His main research interest is energy conservation and environmental protection.